

Ivo SENJANOVIĆ¹
 Neven HADŽIĆ¹
 Dae-Seung CHO²

Influence of Different Restoring Stiffness Formulations on Hydroelastic Response of Large Container Ships

Authors' addresses:

¹University of Zagreb, Faculty of Mechanical Engineering and Naval Architecture, Ivana Lučića 5, 10000 Zagreb, Croatia

e-mail: ivo.senjanovic@fsb.hr

² Pusan National University, San 30 Jangjeon-dong, Guemjeong-gu, Busan, 609-735, Korea

Received (Primljeno): 2012-12-04

Accepted (Prihvaćeno): 2012-12-27

Open for discussion (Otvoreno za raspravu): 2014-09-30

Original scientific paper

Pronounced flexibility of modern container ships can cause falling into resonance with the encounter frequencies of ordinary sea spectrum causing consequently the occurrence of springing. In order to adequately capture such physical phenomena, hydroelasticity methodology for ship structure design has to be applied including the proper definition of the restoring stiffness, being one of the main hydroelastic analysis components. This paper deals with three current restoring stiffness formulations – the consistent one with distributed mass, the consistent one with lumped masses, and the complete one. Formulation of the restoring stiffness via the finite element method is developed as a very useful approach for practical utilization of the hydroelasticity methodology. The validity of the new developed approach is checked on the case of a regular barge. The hydroelasticity of one real life container ship is evaluated and the influence of different restoring stiffness formulations is considered.

Keywords: *container ship, finite element method, geometric stiffness, hydroelasticity, restoring stiffness*

Utjecaj različitih formulacija povratne krutosti na hidroelastični odziv velikih kontejnerskih brodova

Izvorni znanstveni rad

Izražena fleksibilnost trupa suvremenih kontejnerskih brodova može prouzročiti pojavu rezonantnoga gibanja u slučaju uobičajenoga stanja mora i posljedično prouzročiti pojavu pruženja. Kako bi se takva fizikalna pojava adekvatno obuhvatila potrebno je primijeniti metodologiju analize hidroelastičnosti, uključujući i točnu definiciju povratne krutosti koja predstavlja jednu od osnovnih sastavnica analize hidroelastičnosti. Ovaj rad obuhvaća tri aktualne formulacije povratne krutosti: konzistentna s distribuiranom masom, konzistentna s masom koncentriranom u čvorovima modela i cjelokupna formulacija. Prikazana je formulacija povratne krutosti metodom konačnih elemenata, što je vrlo korisno za praktičnu uporabu prigodom provođenja analize hidroelastičnosti. Vjerodostojnost prikazanoga pristupa provjerena je za slučaj pravilne barže. Za ilustraciju je provedena hidroelastična analiza jednoga kontejnerskog broda pri čemu je razmotren utjecaj pojedine formulacije povratne krutosti na ukupni hidroelastični odziv.

Ključne riječi: geometrijska krutost, hidroelastičnost, kontejnerski brod, metoda konačnih elemenata, povratna krutost

1 Introduction

The continuous growth of international maritime transport resulted in designing and building bigger and faster container ships. This development can be characterized as continuous increase in capacity and size. Due to optimized structure, the ship hull of modern ships is quite flexible. As a result the first natural frequencies of such ships are quite low, especially in the case of large container ships due to open cross section and consequently reduced torsional stiffness [1], and can easily fall into resonance with the encounter frequency in an ordinary sea spectrum [2]. Due to that fact, traditional ship strength analysis, based on determination of wave loads on a ship as a rigid body, is not reliable enough [3]. Therefore, it is necessary to perform the ship hydroelastic analysis, which can be defined as fluid-structure interaction type analysis relating external hydrodynamic and internal elastic forces.

Methodology of ship hydroelastic analysis, described in [4], includes definition of structural model with conventional stiffness, mass distribution, restoring stiffness, added mass, damping and wave excitation, and is based on the modal superposition method offering in such way a reduction of the number of equations and computing time [5].

The definition of restoring stiffness, as a part of the methodology of hydroelastic analysis, was found to be quite complex. There are two basic approaches, a pure hydromechanical one and another extended to the structure. In a well-known Price and Wu restoring stiffness formulation [6] only the basic hydrostatic pressure term is taken into account. Newman extended the definition by giving the necessary hydrostatic pressure coefficient [7]. However, these two formulations are not complete, since gravity part is missing. The above shortcoming was eliminated by Riggs, specifying new modal pressure coefficient and adding the gravity term [8]. However, this formulation is not correct due to mixed indices in the restoring stiffness matrix. Similar formulation based on the variational principle and virtual displacements was given by Malenica [9]. Molin [10] derived the same restoring stiffness formula by converting the wetted surface integral into the immersed volume integral in accordance with the Gauss-Ostrogradski theorem [11]. However, these formulations do not satisfy ship's equilibrium in the lower wave frequency domain, where rigid body motion is dominant and the restoring stiffness plays the main role. The reason is that some terms of stiffness matrix are specified as a relation between forces and displacement gradients instead of displacement that follows from the stiffness definition.

2 State-of-the art

Three recent restoring stiffness formulations, presented in Table 1, are written in the ship global coordinate system with origin located in the centroid of water plane. Index notation is used due to the reason of concise presentation, where H_k represents mode

components, $H_{k,l}$ derivatives of mode components, N_k components of normal vector to the wetted surface directed into the body, S wetted surface, V structure volume, g gravity constant, ρ water density, ρ_S structure density, Z depth from the waterplane, i, j mode indices and Σ_{kl} stress tensor.

Table 1 Current formulations of modal restoring stiffness
Tablica 1 Aktualne formulacije povratne krutosti

Contribution from	Notation	Consistent Equation (1) [12, 14]	Complete Equation (2) [13]	Unified Equation (3) [15]
a) Pressure	C_{ij}^P	$\rho g \iint_S H_k^i H_3^j N_k dS$ (1a)	$\rho g \iint_S H_k^i H_3^j N_k dS$ (2a)	$\rho g \iint_S H_k^i H_3^j N_k dS$ (3a)
b) Normal vector and mode	C_{ij}^{nh}	$\rho g \iint_S Z H_k^i H_{l,l}^j N_k dS$ (1b)	$\rho g \iint_S Z H_k^i H_{l,l}^j N_k dS$ (2b)	$\rho g \iint_S Z H_k^i H_{l,l}^j N_k dS$ (3b)
c) Gravity load	C_{ij}^m	$g \iiint_V \rho_S H_k^i H_{3,k}^j dV$ (1c)		
d) Boundary stress (rigid body)	$-k_{ij}^{S0}$		$-\rho g \iint_S Z H_k^i H_{l,l}^j N_k dS$ (2d)	
e) Geometric stiffness	k_{ij}^G		$\iiint_V \Sigma_{kl} H_{m,k}^i H_{m,l}^j dV$ (2e)	$\iiint_V \Sigma_{kl} H_{m,k}^i H_{m,l}^j dV$ (3e)
f) Boundary stress (elastic body)	$-k_{ij}^{SZ}$			$\rho g \iint_S Z H_k^i H_{l,k}^j N_k dS$ (3f)
g) Structural deformation	$C_{ij}^m - k_{ij}^{VZ}$			$g \iiint_V \rho_S H_k^i \left(H_{3,k}^j + H_{k,3}^j \right) dV$ (3g)

Development of the current restoring stiffness formulations and their relationship are shown in Figure 1. Consistent restoring stiffness, Eq. (1) in Table 1, derived for ship structures, is based on variational principle and the method of virtual displacements [12].

Formulation of Huang and Riggs [13], Eq. (2) in Table 1, called complete restoring stiffness, takes pressure change into account due to variation of depth and direction caused by structure deformation as well as the geometric stiffness based on still water stress distribution. The gravity term is indirectly included as a rigid body part of geometric stiffness. This formulation is suitable for general off-shore structures where geometric stiffness plays a dominant role and it results with symmetric restoring stiffness matrix. The Huang and Riggs formula can be transformed and reduced to the form of Eq. (1) in Table 1 [14].

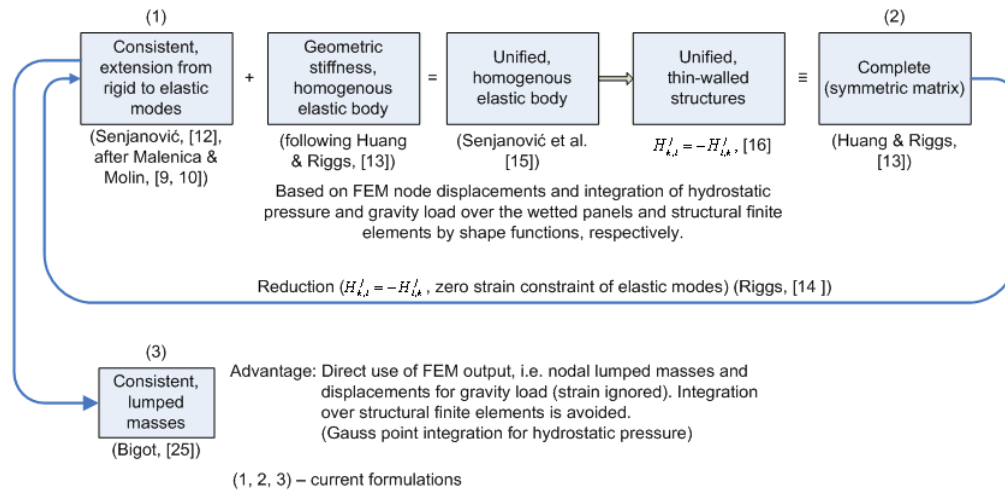


Figure 1 **Current restoring stiffness formulations**
 Slika 1 **Aktualne formulacije povratne krutosti**

The third formulation of restoring stiffness, Eq. (3) in Table 1, is obtained by unifying the consistent restoring stiffness, Eq. (1), and geometric stiffness, Eq. (2e), since they have some common terms, [15]. As a result the term $-k_{ij}^{SZ}$, Eq. (3f), occurs instead of $-k_{ij}^{S0}$, Eq. (2d), and also the new term $C_{ij}^m - k_{ij}^{VZ}$, Eq. (3g), appears. It was found in [16, 17] that unified restoring stiffness is not applicable in the case of thin-walled structures, since mode derivatives $H_{l,k}^j$ and $H_{3,k}^j$ are not completely available in that case, Figure 2.

Up to now, consistent restoring stiffness has been used for hydroelastic analysis of barges in model tests, ship beam model, and for 3D FEM model of real ship structure in an appropriate way [18, 19, 20], while the complete one has been employed for barge hydroelastic analysis and simplified analysis of the Wigley ship form [21]. Unified restoring stiffness has been employed in the analytical solution for restoring stiffness in a barge hydroelastic analysis [16, 22, 23].

The objective of this article is to investigate the impact of different restoring stiffness formulations on the hydroelastic response of a real container ship structure in order to establish the required level of restoring stiffness complexity and to give recommendations for further practical usage. The three current formulations that are considered here are given in Figure 1 as consistent formulation with distributed mass, [12], consistent formulation with lumped mass, and complete restoring stiffness formulation [13].

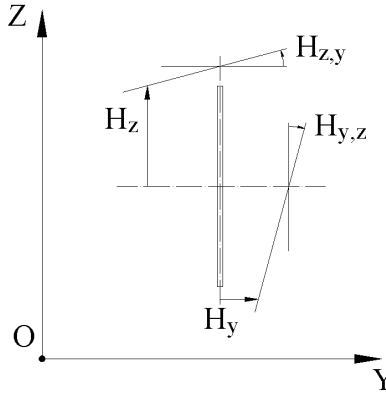


Figure 2 Relation between mode derivatives ($H_{z,y} = -H_{y,z}$ for rigid body)

Slika 2 Odnos derivacija modalnih pomaka ($H_{z,y} = -H_{y,z}$ za kruto tijelo)

3 Integration of stiffness coefficients

Integration of stiffness coefficients over the panels of the wetted surface can be performed either using the structural or the coarse hydrodynamic mesh, normally applied in the hydrodynamic analysis procedure. The latter is preferred due to computing time reduction but some difficulties arise since it is necessary to interpolate modal displacements from structural nodes to the new panel nodes and to determine approximately the corresponding modal derivatives [24]. This is especially pronounced in the case of geometric stiffness, where the stress tensor Σ_{kl} in global coordinate system is not known explicitly.

In order to perform a more reliable and accurate numerical integration of the surface and volumetric stiffness coefficients it is necessary to transform all involved quantities from the global to local coordinate system, and use shape functions for their distribution within the structural finite elements mesh [25].

3.1 Pressure coefficient, Eqs. (1a, 2a)

The pressure coefficient expressed in index notation can be presented in matrix notation as

$$C_{ij}^p = \rho g \iint_S \langle N_x \ N_y \ N_z \rangle \begin{Bmatrix} H_x^i \\ H_y^i \\ H_z^i \end{Bmatrix} H_z^j dS. \quad (4)$$

By applying the well known finite element relations using transformation matrix, (A2), and shape functions [25], after some rearrangement the pressure coefficient can be expressed as

$$C_{ij}^p = \rho g \langle N_x \ N_y \ N_z \rangle \sum_{k=1}^M \sum_{l=1}^M \begin{Bmatrix} H_{x,k}^i \\ H_{y,k}^i \\ H_{z,k}^i \end{Bmatrix} H_{z,l}^j \iint_S \phi_k \phi_l \, dS, \quad (5)$$

where k and l are nodal indices. The shape functions, ϕ_k and ϕ_l , are defined in the local coordinate system and can be integrated analytically for simple panels or numerically by Gauss points [25]. All the other quantities in (5) are related to the global coordinate system.

3.2 Normal vector and mode coefficient, Eqs. (1b, 2b)

This coefficient can be presented in matrix notation as follows

$$C_{ij}^{nh} = \rho g \iint_S Z \langle N_x \ N_y \ N_z \rangle \begin{Bmatrix} H_x^i \\ H_y^i \\ H_z^i \end{Bmatrix} \left\langle \frac{\partial}{\partial X} \ \frac{\partial}{\partial Y} \ \frac{\partial}{\partial Z} \right\rangle \begin{Bmatrix} H_x^j \\ H_y^j \\ H_z^j \end{Bmatrix} dS. \quad (6)$$

By taking into account basic finite element relations, the shape functions can be grouped in the integrand

$$C_{ij}^{nh} = \rho g \langle N_x \ N_y \ N_z \rangle \sum_{k=1}^M \sum_{l=1}^M \begin{Bmatrix} H_{x,k}^i \\ H_{y,k}^i \\ H_{z,k}^i \end{Bmatrix} \langle H_{x,l}^j \ H_{y,l}^j \ H_{z,l}^j \rangle [c]^T \iint_S Z \phi_k \begin{Bmatrix} \frac{\partial \phi_l}{\partial x} \\ \frac{\partial \phi_l}{\partial y} \\ \frac{\partial \phi_l}{\partial z} \end{Bmatrix} dS. \quad (7)$$

3.3 Boundary stress coefficient, Eq. (2d)

This coefficient written in matrix notation reads

$$-k_{ij}^{S0} = -\rho g \iint_S Z \langle H_x^i \ H_y^i \ H_z^i \rangle \begin{Bmatrix} \frac{\partial}{\partial X} \\ \frac{\partial}{\partial Y} \\ \frac{\partial}{\partial Z} \end{Bmatrix} \langle H_x^j \ H_y^j \ H_z^j \rangle \begin{Bmatrix} N_x \\ N_y \\ N_z \end{Bmatrix} dS. \quad (8)$$

By taking into account finite element relations, and after some rearrangement one finds

$$-k_{ij}^{S0} = -\rho g \langle N_x \ N_y \ N_z \rangle \sum_{k=1}^M \sum_{l=1}^M \begin{Bmatrix} H_{x,l}^j \\ H_{y,l}^j \\ H_{z,l}^j \end{Bmatrix} \langle H_{x,k}^i \ H_{y,k}^i \ H_{z,k}^i \rangle [c]^T \iint_S Z \phi_k \begin{Bmatrix} \frac{\partial \phi_l}{\partial x} \\ \frac{\partial \phi_l}{\partial y} \\ \frac{\partial \phi_l}{\partial z} \end{Bmatrix} dS. \quad (9)$$

3.4 Coefficient of gravity load, Eq. (1c) – distributed mass

The ship structure is modeled with shell finite elements of thickness h , so the volume integral in Eq. (1c) is reduced to the surface one, which can be written in matrix notation

$$C_{ij}^m = g \rho_S h \iint_S \langle H_x^i \ H_y^i \ H_z^i \rangle \begin{Bmatrix} \frac{\partial}{\partial X} \\ \frac{\partial}{\partial Y} \\ \frac{\partial}{\partial Z} \end{Bmatrix} H_z^j dS. \quad (10)$$

If the mode displacements are expressed by nodal displacements and shape functions [25], one obtains

$$C_{ij}^m = \rho_S g h \sum_{k=1}^M \sum_{l=1}^M \langle H_{x,k}^i \ H_{y,k}^i \ H_{z,k}^i \rangle H_{z,l}^j [c]^T \iint_S \phi_k \begin{Bmatrix} \frac{\partial \phi_l}{\partial x} \\ \frac{\partial \phi_l}{\partial y} \\ \frac{\partial \phi_l}{\partial z} \end{Bmatrix} dS. \quad (11)$$

3.5 Coefficient of gravity load, Eq. (1c) – lumped mass

Concentrated mass elements are commonly used for modeling of ship cargo and equipment and they have to be taken into account within the volumetric integral of gravity load coefficient. Eq. (1c) expressed in expanded form [26],

$$C_{ij}^m = gm \left(H_x^i \frac{\partial H_z^j}{\partial X} + H_y^i \frac{\partial H_z^j}{\partial Y} + H_z^i \frac{\partial H_z^j}{\partial Z} \right), \quad (12)$$

takes into account modal displacements, rotations and strain. By neglecting strain deformation terms and taking into account only the rotation component, the coefficient of gravity load for lumped mass can be expressed as

$$C_{ij}^m = gm \left[H_x^i \frac{1}{2} (-\alpha_y - \beta_y) + H_y^i \frac{1}{2} (\alpha_x + \beta_x) \right], \quad (13)$$

where α_x , α_y , β_x and β_y are angles of rotation about x and y axis respectively, Figure 3.

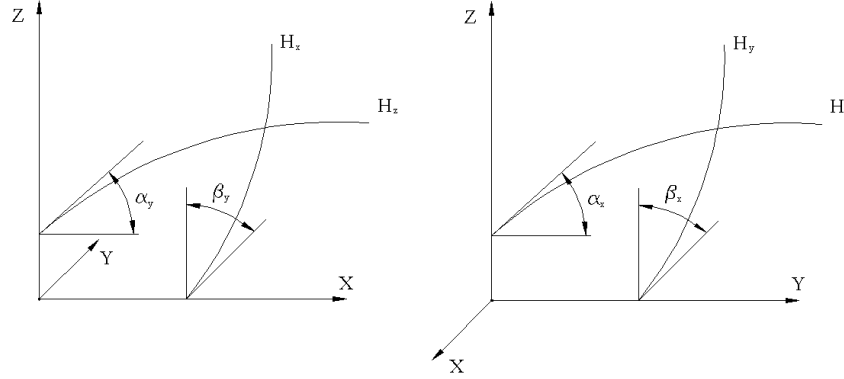


Figure 3 Angles of rotation about x and y axis
Slika 3 Kutovi zakreta oko x i y osi

3.6 Geometric stiffness, Eq. (2e)

Geometric stiffness, as well as the other restoring stiffness coefficients, represents energy which does not depend on the chosen coordinate system. Hence, the local coordinate system is used in this case due to easier derivation of geometric stiffness of finite element. The corresponding equation (2e) for an element written in matrix in the local coordinate system notation takes the form

$$k_{ij}^G = h \sum_m \iint_S \langle h_{m,k}^i \rangle [\sigma_{kl}] \{ h_{m,l}^j \} dS, \quad (14)$$

where σ_{kl} are elements of stress matrix due to preloading in calm sea and m indicates mode components in x , y and z direction. After some rearrangement by applying finite element and well known mathematical relations [16, 25, 27] the geometric stiffness coefficient takes the final form

$$k_{ij}^G = h \sum_{k=1}^M \sum_{l=1}^M \left(\langle c \rangle_x [H_{kl}^{ij}] \{ c \}_x + \langle c \rangle_y [H_{kl}^{ij}] \{ c \}_y + \langle c \rangle_z [H_{kl}^{ij}] \{ c \}_z \right) \cdot \left(I_{11}^{kl} \sigma_{xx} + I_{21}^{kl} \sigma_{yx} + I_{12}^{kl} \sigma_{xy} + I_{22}^{kl} \sigma_{yy} \right), \quad (15)$$

where

$$\begin{aligned}
I_{11}^{kl} &= \iint_S \frac{\partial \phi_k}{\partial x} \frac{\partial \phi_l}{\partial x} dS, \\
I_{21}^{kl} &= \iint_S \frac{\partial \phi_k}{\partial y} \frac{\partial \phi_l}{\partial x} dS, \\
I_{12}^{kl} &= \iint_S \frac{\partial \phi_k}{\partial x} \frac{\partial \phi_l}{\partial y} dS, \\
I_{22}^{kl} &= \iint_S \frac{\partial \phi_k}{\partial y} \frac{\partial \phi_l}{\partial y} dS.
\end{aligned} \tag{16}$$

If the local coordinate system coincides with the global one, directional coefficients $\cos(x, X) = \cos(y, Y) = \cos(z, Z) = 1$, while the remaining coefficients for combined axis are zero, expression (15) is reduced to the simpler form

$$k_{ij}^G = h \sum_{k=1}^M \sum_{l=1}^M (H_{x,k}^i H_{x,l}^j + H_{y,k}^i H_{y,l}^j + H_{z,k}^i H_{z,l}^j) (I_{11}^{kl} \sigma_{xx} + I_{21}^{kl} \sigma_{yx} + I_{12}^{kl} \sigma_{xy} + I_{22}^{kl} \sigma_{yy}). \tag{17}$$

Three terms exist in the first bracket and if one considers a finite element in xy plane, then the first two terms include membrane (in plane) displacements in x and y direction, while the third term is related to the element deflection in z direction. Hence, the third term is related to the ordinary geometric stiffness used in stability analysis, and therefore is not sufficient alone for hydroelastic analysis [16, 26]. The formulation of all derived coefficients for the case of three node triangular, four node rectangular, and two node beam elements is given in [16, 17].

4 Description of the computer program

The program is developed for the ship hydroelastic analysis which is based on the modal superposition method, in order to reduce the number of differential equations of motion of the discretized structure and wetted surface. The dry natural modes of ship structure are used and they are determined by solving the eigenvalue problem formulated by the finite element method

$$([K] - \Omega^2 [M])\{H\} = \{0\}, \tag{18}$$

where $[K]$ is the stiffness matrix, $[M]$ is the mass matrix, $\{H\}$ is a mode vector and Ω is a dry natural frequency.

The modal differential equation of ship hydroelastic analysis in frequency domain reads

$$\{([k] + [C]) - i\omega([d] + [B(\omega)]) - \omega^2([m] + [A(\omega)])\}\{\xi\} = \{F(\omega)\}, \tag{19}$$

where $[k]$ is structural stiffness matrix, $[d]$ structural damping matrix, $[m]$ structural mass matrix, $[C]$ restoring stiffness matrix, $[B(\omega)]$ hydrodynamic damping matrix,

$[A(\omega)]$ added mass matrix, $\{\xi\}$ modal amplitude vector, $\{F\}$ wave excitation vector and ω encounter frequency.

The integrated program for ship hydroelastic analysis consists of several modules. NASTRAN [28] is applied for 3D modeling of ship structure and calculation of dry natural vibrations, i.e. natural frequencies and modes, Eq. (18). This program is also used for ship strength calculation in calm water in order to determine the membrane stresses in geometric stiffness matrix. Newly developed software, RESTAN, is applied for the calculation of modal restoring stiffness. For determination of hydrodynamic coefficients, i.e. modal added mass, damping and wave excitation program HYDROSTAR [29] is used and final modal ship motion equation (19) is solved using program MFRT.

Program RESTAN (REstoring STiffness ANalysis) is used for calculating the restoring stiffness coefficients according to the formulae worked out in the previous section. Hence, there are two types of formulae; one set obtained by volume integration over the ship structure, and another over the wetted surface. For the integration needs the necessary data generated by NASTRAN are used: node ordinary number and coordinates, ordinary number and nodes of the finite elements, material characteristics, components of modal displacements, stress components for ship in calm sea, etc. The wetted surface panels are taken from the 3D FEM model. Only wetted part of the panels intersected by the waterline is included in the wetted surface model.

5 Test example

The application of the developed finite element formulation of restoring stiffness coefficients is tested in the case of a prismatic thin-walled barge, since in this case the restoring stiffness for rigid body modes can be determined analytically in order to verify the analysis procedure. The main particulars of the barge are the following:

Length	$L = 150$ m
Breadth	$B = 24$ m
Draught	$T = 6$ m
Depth	$D = 15$ m
Displacement	$\Delta = 22140$ t
Vertical position of center of gravity	$z_G = 7.5$ m
Waterplane area	$A_{WL} = 3600$ m ²
Water density	$\rho = 1.025$ t/m ³

As shown in Figure 4, the inner barge structure consists of three longitudinal and 24 transverse bulkheads, and four decks. Thickness of all structural elements is 10 mm. The barge mass distribution is determined by specifying the density of the structural elements. In order to impose some vertical bending of the barge in calm sea, the density for elements in the aft and fore region of 36 m length is set to $\rho_1 = 0.260427$ t/m³, while in the middle region of 78 m length the density is set to $\rho_2 = 0.781277$ t/m³.

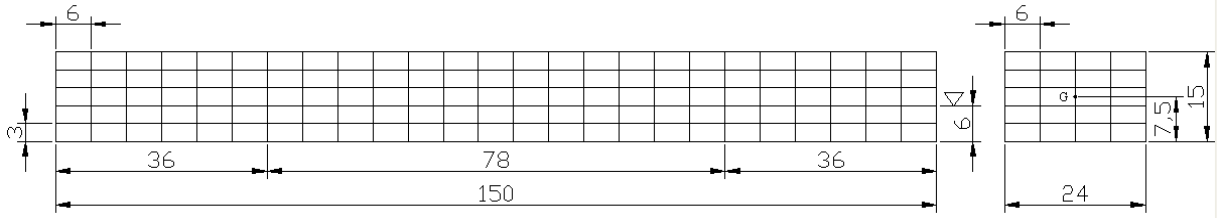


Figure 4 Thin-walled barge structure
Slika 4 Struktura tankostijene barže

The finite element mesh coincides with the topology of the barge structure in order to minimize local deformations vs. girder ones. Longitudinal strength in calm water is performed by program NASTRAN. The barge still water sagging with the associated stress distribution is shown in Figure 5. The maximum stress occurs in the bottom and upper deck at the midship section, $\sigma_{\max} = \pm 137.5 \text{ N/mm}^2$.

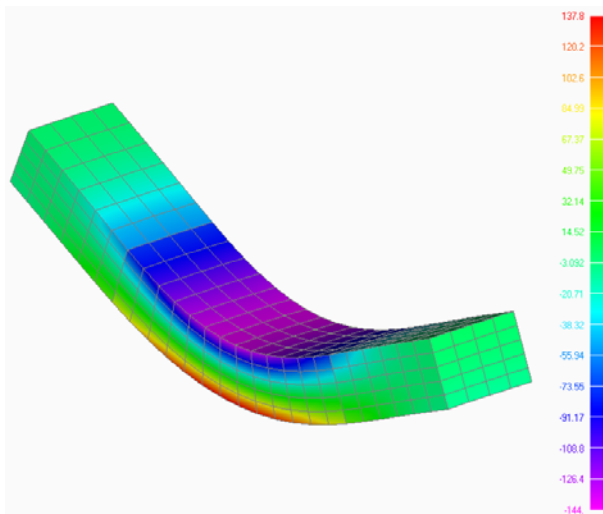


Figure 5 Stress distribution in calm sea, prismatic barge
Slika 5 Raspodjela naprezanja na mirnoj vodi, prizmatična barža

The free vibration calculation is also performed by NASTRAN for the same mass distribution as specified above. The natural frequencies of the first four vertical, horizontal, and torsional modes are listed in Table 2.

Table 2 Natural frequencies of prismatic barge, Ω , [Hz]

Tablica 2 Prirodne frekvencije prizmatične barže, Ω , [Hz]

Mode	Vertical	Horizontal	Torsional
1	1.4611	2.1674	2.9425
2	3.1266	4.5227	5.4358
3	5.3028	7.5194	7.4517
4	7.7376	10.8088	9.5297

The first mode of each vibration type is shown in Figures 6, 7 and 8. No coupling between horizontal and torsional vibrations is encountered in this case, since the torsional and gravity centre are the same point.

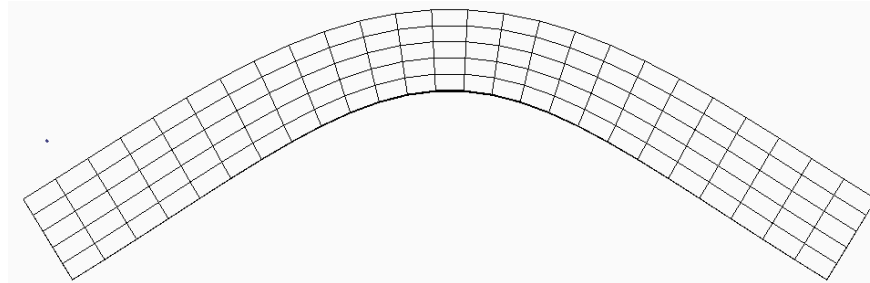


Figure 6 The first vertical mode, prismatic barge
Slika 6 Prvi vertikalni prirodni oblik vibriranja, prizmatična barža

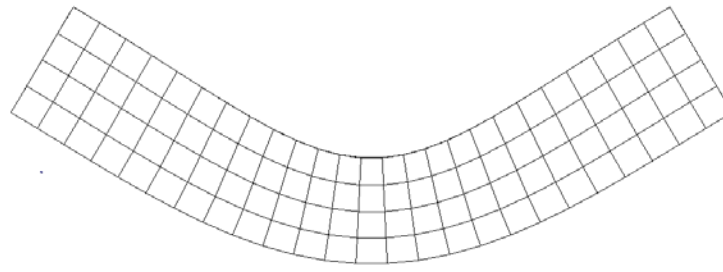


Figure 7 The first horizontal mode, prismatic barge
Slika 7 Prvi horizontalni prirodni oblik vibriranja, prizmatična barža

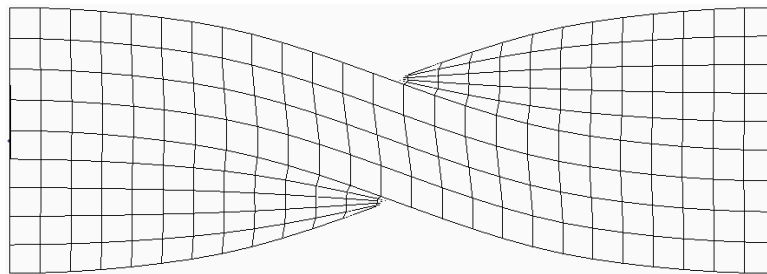


Figure 8 The first torsional mode, prismatic barge
Slika 8 Prvi tozijski prirodni oblik vibriranja, prizmatična barža

Three numerical calculations of restoring stiffness are performed. The first one is for the consistent stiffness with distributed structural mass, Eq. (1). The second calculation is also performed for the consistent stiffness, but the gravity coefficient, C_{ij}^m , Eq. (1c), is determined by employing the fully lumped masses (without the rotational components). The third calculation deals with the complete restoring stiffness, Eq. (2). The calculated coefficients and the resulting stiffness are listed in Table 3. The following units are used in all calculations: N, m, s, kg.

Table 3 Restoring stiffness coefficients of prismatic barge, C
 Tablica 3 Koeficijenti povratne krutosti prizmatične barže, C

Motion	Formulation	C_{ij}^p	C_{ij}^{nh}	C_{ij}^m	$-k_{ij}^{S0}$	k_{ij}^G	C_{ij}^{total}	C_{ij}^{an}	$\varepsilon(\%)$
Heave $i=j=3$	Consistent dist. mass	$3.6199 \cdot 10^7$	0.0	0.0			$3.6199 \cdot 10^7$	$3.6190 \cdot 10^7$	0.025
	Consistent lumped mass	$3.6199 \cdot 10^7$	0.0				$3.6199 \cdot 10^7$		0.025
	Complete	$3.6199 \cdot 10^7$	0.0				$3.6199 \cdot 10^7$		0.025
Roll $i=j=4$	Consistent dist. mass	$7.6018 \cdot 10^8$	0.0	0.0			$7.6018 \cdot 10^8$	$7.601 \cdot 10^8$	0.010
	Consistent lumped mass	$7.6018 \cdot 10^8$	0.0						
	Complete	$7.6018 \cdot 10^8$	0.0		$2.2805 \cdot 10^9$	$-2.2806 \cdot 10^9$	$7.6015 \cdot 10^8$		0.007
Pitch $i=j=5$	Consistent dist. mass	$6.6896 \cdot 10^{10}$	0.0	0.0			$6.6896 \cdot 10^{10}$	$6.6890 \cdot 10^{10}$	0.009
	Consistent lumped mass	$6.6896 \cdot 10^{10}$	0.0						
	Complete	$6.6896 \cdot 10^{10}$	0.0		$2.2805 \cdot 10^9$	$-2.2806 \cdot 10^9$	$6.6896 \cdot 10^{10}$		0.009

For heave only pressure coefficient C_{33}^p is relevant. Almost the exact value is obtained in all three calculations, $\varepsilon = 0.025\%$. For roll motion, the pressure coefficient C_{44}^p has the main contribution. Since reference point coincides with the centre of gravity, the coefficients C_{44}^{nh} and C_{44}^m are zero. The value of C_{44}^{tot} for roll is very close to the exact value, $\varepsilon = 0.01\%$. In the complete restoring stiffness it is obvious that $-k_{44}^{S0} + k_{44}^G \approx 0$ as it is expected since that expression has to compensate C_{44}^m which is equal to zero. Discrepancy of the total coefficient, $\varepsilon = 0.007\%$, is very small. Pitch restoring is not as sensitive as that of roll, so discrepancies in all three cases are considerably smaller.

Hydroelastic response of the considered barge is determined for the case of heading angle $\chi = 150^\circ$ (following waves $\chi = 0^\circ$). A large number of wave frequencies in the range from 0.1 to 1.5 rad/s, with step $\Delta\omega = 0.02$ rad/s is taken into account.

In the following figures transfer functions of sectional forces are shown. Moments are related to the midship section, while shear forces are determined at the aft section $0.25L$, where it is expected to have maximum values. The RAO of the vertical bending moment, Figure 9, achieves peak value at $\omega = 0.605$ rad/s. The response curves for all three restoring stiffness formulations are the same. RAO of vertical shear force, Figure 10, manifests peak at $\omega = 0.63$ rad/s. The response curves are very close to each other.

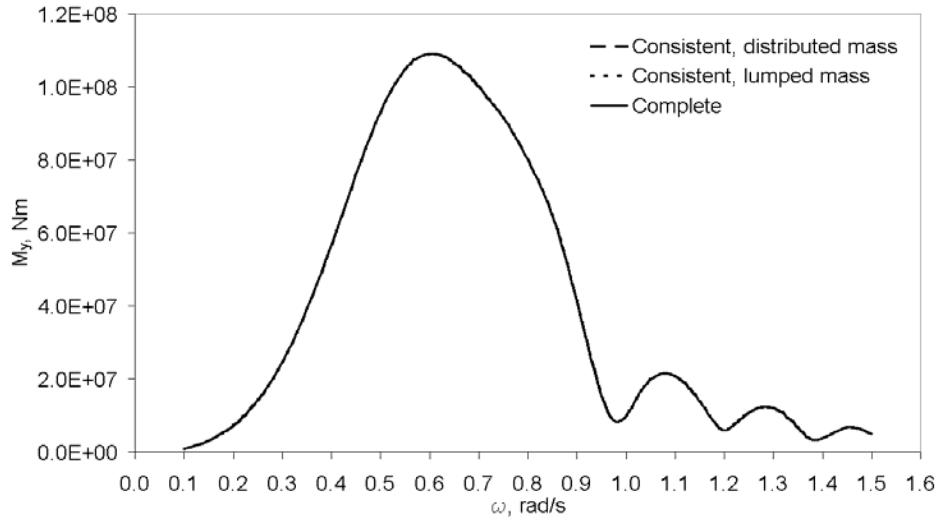


Figure 9 Transfer function of vertical bending moment at midship section, prismatic barge, $\chi = 150^\circ$
 Slika 9 Prijenosna funkcija vertikalnog momenta savijanja na sredini, prizmatična barža, $\chi = 150^\circ$

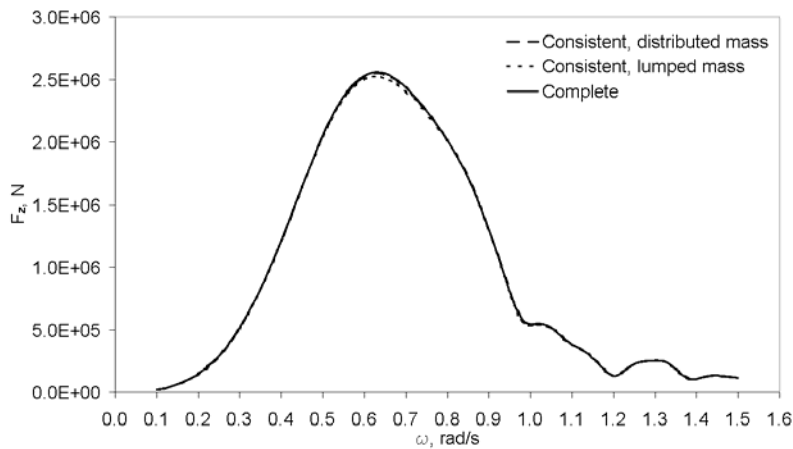


Figure 10 Transfer function of vertical shear force, prismatic barge, $\chi = 150^\circ$, $x = 37.5$ m
 Slika 10 Prijenosna funkcija vertikalne smične sile, prizmatična barža, $\chi = 150^\circ$, $x = 37.5$ m

The RAO of the horizontal bending moment is shown in Figure 11. The maximum peak occurs at $\omega = 0.78$ rad/s. There are some differences of the response curves at the first peak at $\omega = 0.52$ rad/s, while elsewhere in the frequency region the response is the same. That is similar for the RAO of the horizontal shear force, Figure 12. In ship hydroelastic analysis the most interesting RAO is that of torsional moment. In the considered case maximum value occurs at $\omega = 0.575$ rad/s, and response curves determined by different restoring stiffness formulations follow each other very well, Figure 13.

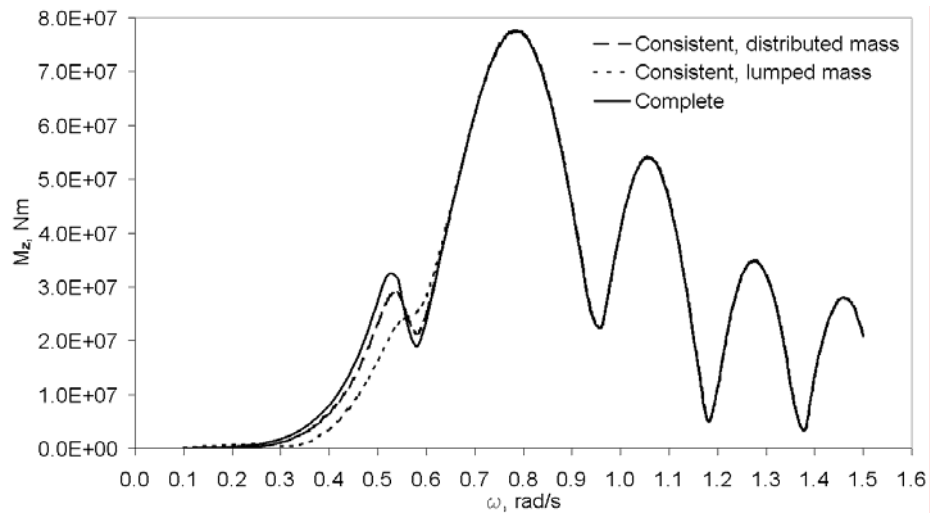


Figure 11 Transfer function of the horizontal bending moment at midship section, prismatic barge, $\chi = 150^\circ$
 Slika 11 Prijenosna funkcija horizontalnog momenta savijanja na sredini, prizmatična barža $\chi = 150^\circ$

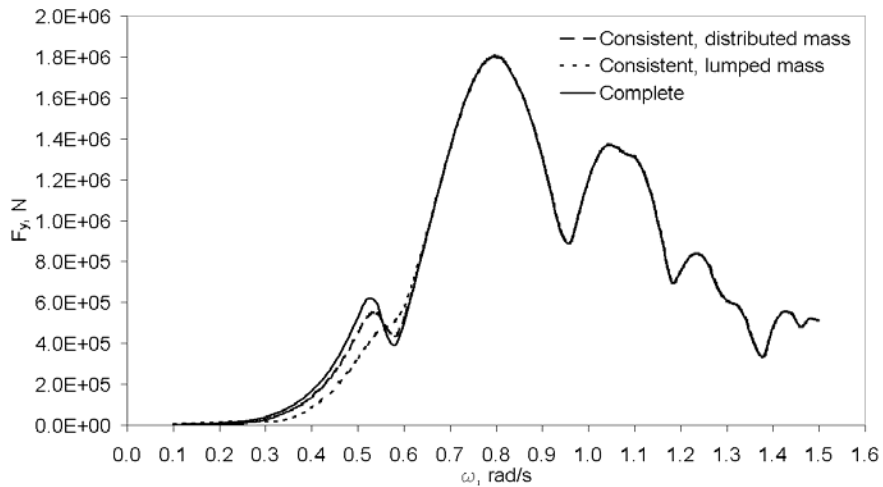


Figure 12 Transfer function of the horizontal shear force, prismatic barge, $\chi = 150^\circ$, $x = 37.5$ m
 Slika 12 Prijenosna funkcija horizontalne smične sile, prizmatična baža, $\chi = 150^\circ$, $x = 37.5$ m

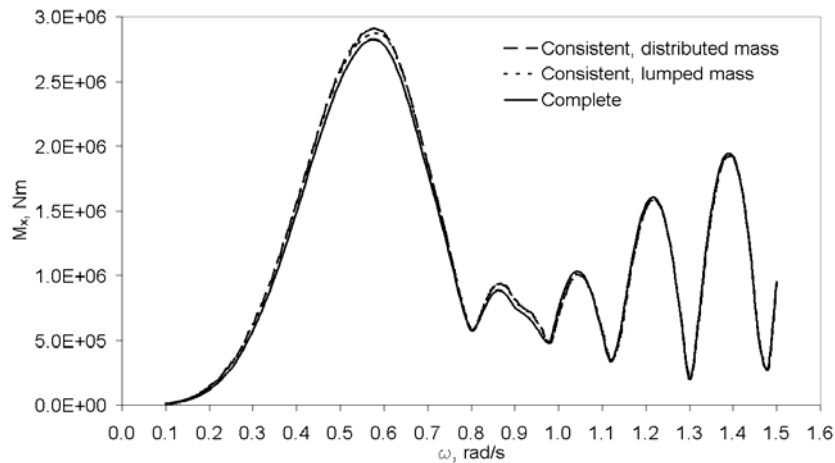


Figure 13 Transfer function of the torsional moment at midship section, prismatic barge, $\chi = 150^\circ$

Slika 13 Prijenosna funkcija momenta uvijanja na sredini, prizmatična baža, $\chi = 150^\circ$

6 Illustrative example

The application of the developed finite element formulation of restoring stiffness coefficients is illustrated in a case of a real container ship whose main particulars are the following:

Length over all	$L_{oa} = 349.00$ m
Length between perpendiculars	$L_{pp} = 333.44$ m
Breadth	$B = 42.80$ m
Draught	$T = 13.10$ m
Depth	$D = 27.30$ m
Displacement	$\Delta = 125604$ t
Water density	$\rho = 1.025$ t/m ³
Capacity	9415 TEU
Speed	$v = 25$ kn

General arrangement of a 9415 TEU container ship is shown in Figure 14. 3D FEM model, consisting of 84893 elements and 16966 structural nodes, was generated in program NASTRAN with the purpose of performing the ship still water strength and free vibration analysis. Container cargo was modeled using the concentrated mass elements rigidly connected with the surrounding structural nodes. In such a way sectional cargo mass is lumped in its center of gravity.

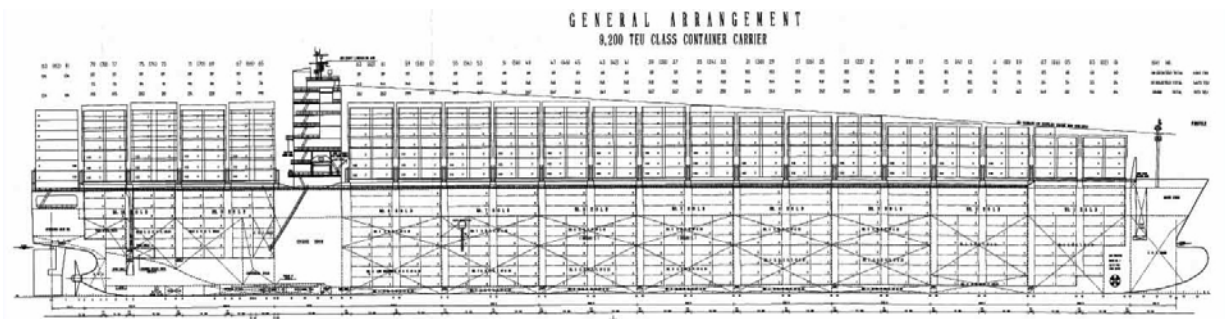


Figure 14 General arrangement of a 9415 TEU container ship
Slika 14 Opći plan kontejnerskog broda kapaciteta 9415 TEU

The ship hogging in calm sea with stress distribution is shown in Figure 15. Natural frequencies of the first six dry natural modes are listed in Table 4, while the first two coupled horizontal and torsional modes and the first vertical mode are shown in Figures 16 and 17 respectively.

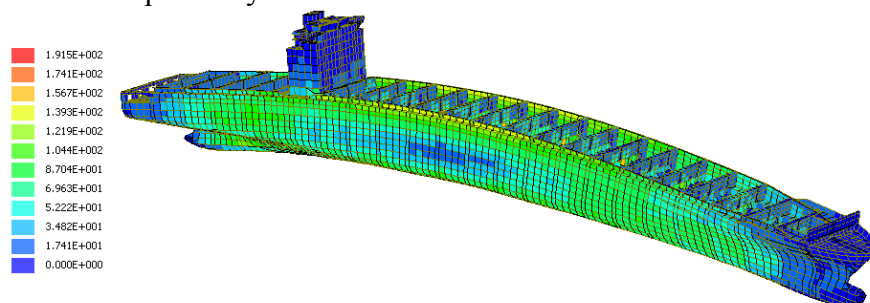


Figure 15 Von Mises stress distribution in calm sea, a 9415 TEU container ship
Slika 15 Razdioba von Mises naprezanja na mirnom moru, kontejnerski brod kapaciteta 9415 TEU

Table 4 Natural frequencies of a 9415 TEU container ship, Ω , [Hz]

Tablica 4 Prirodne frekvencije kontejnerskog broda kapaciteta 9415 TEU, Ω [Hz]

Mode no.	Description	f_i , [Hz] f [Hz]
1	H1+T1	0.415
2	H1+T2	0.588
3	V1	0.676
4	H2+T3	1.018
5	V2	1.384
6	H3+T4	1.391

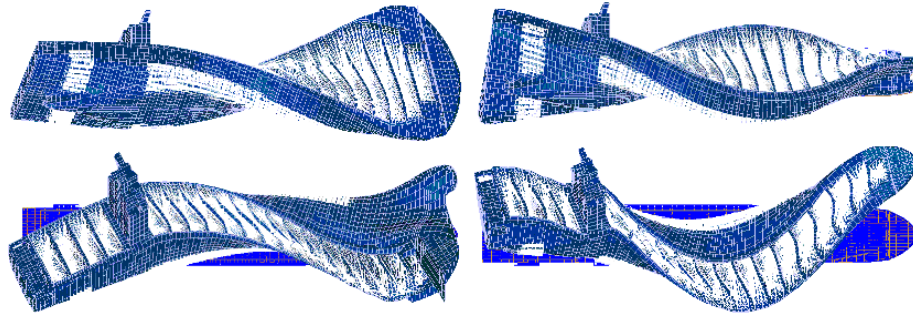


Figure 16 The first and the second coupled torsional and horizontal mode shapes (lateral and bird's view), a 9415 TEU container ship

Slika 16 Prvi i drugi spregnuti horizontalni i torzijski prirodni oblik vibriranja (bočni i ptičji pogled), kontejnerski brod kapaciteta 9415 TEU

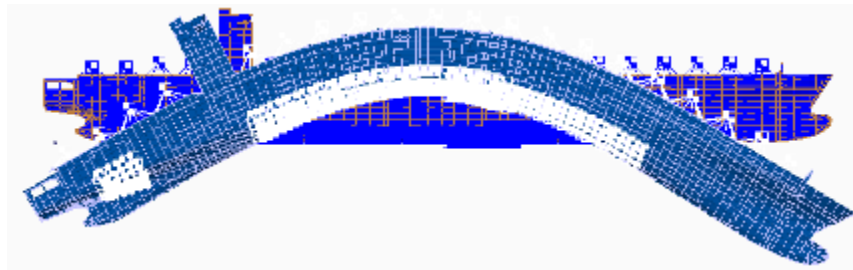


Figure 17 The first vertical mode, a 9415 TEU container ship

Slika 17 Prvi vertikalni prirodni oblik vibriranja, kontejnerski brod kapaciteta 9415 TEU

Three numerical calculations of restoring stiffness are performed, as described in section 5. Validation of the calculations can be checked in the case of heave, roll and pitch since the restoring stiffness for these three motions can be determined analytically using the well known seakeeping restoring stiffness expressions [3]. The calculated coefficients and the resulting stiffness are listed in Table 5. The following units are used in all calculations: N, m, s, kg.

For heave only pressure coefficient C_{33}^p is relevant. Almost the exact value is obtained in all three calculations, $\varepsilon = 1.067\%$ for the first and third formulation, and $\varepsilon = 0.638\%$ in the case of the second one.

Slightly larger disagreement between calculated and analytical value is obtained in the case of roll, i.e. $\varepsilon = -1.575\%$ for consistent, and $\varepsilon = 1.457\%$ for consistent formulation with lumped masses. Special attention has to be given to the restoring stiffness coefficient in the case of complete formulation, since boundary stress coefficient, k_{44}^{S0} , and geometric stiffness coefficient, k_{44}^G , are two close values that cancel each other [16, 17] and in the case of ship structure they are for one order of magnitude greater than the pressure coefficient. Also, due to high complexity of the geometric stiffness coefficient calculation and its dependence on the ship strength analysis it is not possible to achieve close values of those two coefficients, i.e. the real value obtained in the case of roll is $k_{44}^G = -2.9902 \cdot 10^{10}$, which is only 3% larger comparing to the value of the boundary stress coefficient. Therefore, even a small difference between these two coefficients causes significant error in the value of the total restoring coefficients and

consequently making the complete formulation, although physically correct, numerically unstable. To enable adequate comparison of the achieved results the final value of the geometric stiffness coefficient in the case of complete formulation was calibrated with respect to roll in order to cancel the contribution of the boundary stress coefficient.

Table 5 Restoring stiffness coefficients of a 9415 TEU container ship, C
 Tablica 5 Koeficijenti povratne krutosti kontejnerskog broda kapaciteta 9415 TEU, C

Motion	Formulation	C_{ij}^p	C_{ij}^{nh}	C_{ij}^m	$-k_{ij}^{s0}$	k_{ij}^G	C_{ij}^{total}	C_{ij}^{an}	$\varepsilon(\%)$
Heave $i=j=3$	Consistent dist. mass	$1.2027 \cdot 10^8$					$1.2027 \cdot 10^8$	$1.1900 \cdot 10^8$	1.067
	Consistent lumped mass	$1.1976 \cdot 10^8$					$1.1976 \cdot 10^8$		0.638
	Complete	$1.2027 \cdot 10^8$					$1.2027 \cdot 10^8$		1.067
Roll $i=j=4$	Consistent dist. mass	$1.7209 \cdot 10^9$	$-3.9588 \cdot 10^7$	$-1.9863 \cdot 10^7 *$			$1.6614 \cdot 10^9$	$1.6880 \cdot 10^9$	-1.575
	Consistent lumped mass	$1.7346 \cdot 10^9$	0.0	$-2.1990 \cdot 10^7$			$1.7126 \cdot 10^9$		1.457
	Complete	$1.7209 \cdot 10^9$	$-3.9588 \cdot 10^7$		$2.9021 \cdot 10^{10}$	$-2.9026 \cdot 10^{10} *$	$1.6820 \cdot 10^9$		-0.355
Pitch $i=j=5$	Consistent dist. mass	$8.3199 \cdot 10^{11}$	$1.3976 \cdot 10^8$	$2.7184 \cdot 10^8$			$8.3240 \cdot 10^{11}$	$8.2020 \cdot 10^{11}$	1.487
	Consistent lumped mass	$8.1667 \cdot 10^{11}$	0.0	$2.1990 \cdot 10^7$			$8.1669 \cdot 10^{11}$		-0.428
	Complete	$8.3199 \cdot 10^{11}$	$1.3976 \cdot 10^8$		$2.8805 \cdot 10^{10}$	$2.9322 \cdot 10^{10}$	$8.3073 \cdot 10^{11}$		1.283

*Calibrated value

Except that, special care has to be taken in the case of gravity coefficient, C_{44}^m . It can easily be shown that in the case of rigid body modes and when the center of gravity is taken as the reference point, Eq. (1c) yields zero value. This condition is easily achieved in the case of simpler structures like prismatic barge [16] and it is also approximately satisfied in the case of a complex structure with continuous or lumped mass. Some problems arise with the combined continuous and lumped mass approach, making the gravity coefficient very sensitive to mass modeling. Due to that fact, the value of gravity coefficient was also calibrated by correcting the vertical position of the center of gravity of the chosen concentrated cargo. In such way, the original value of $C_{44}^m = -1.714 \cdot 10^8$ was reduced to $C_{44}^m = -1.9863 \cdot 10^7$, which is negligible, comparing to the value of pressure coefficient, $C_{44}^p = 1.7209 \cdot 10^9$, Table 5. Restoring stiffness in the case of pitch is not as sensitive as in the case of roll, and all the achieved values are close to the analytical ones.

Hydroelastic response of the considered container ship was determined for the case of heading angle $\chi = 150^\circ$ (following waves $\chi = 0^\circ$) and for the same range of frequencies as in the case of regular barge. Moments are related to the midship section, while shear forces are determined at the aft section $0.25L$, where it is expected to have maximum values. RAO of the vertical bending moment, Figure 18, achieves significant peak value at $\omega = 0.72$ rad/s. The response curves for all three restoring stiffness formulations are the same. RAO of vertical shear force, Figure 19, manifests the first peak at $\omega = 0.78$ rad/s. The response curves are very close to each other. RAO of horizontal bending moment is shown in Figure 20. The significant peak occurs at $\omega = 0.91$ rad/s with good agreement between all formulations. That is similar for the RAO of the horizontal shear force, Figure 21. In the case of torsional moment RAO,

Figure 22, the first significant peak occurs at $\omega = 1.25$ rad/s, and response curves determined by different restoring stiffness formulations follow each other very well.

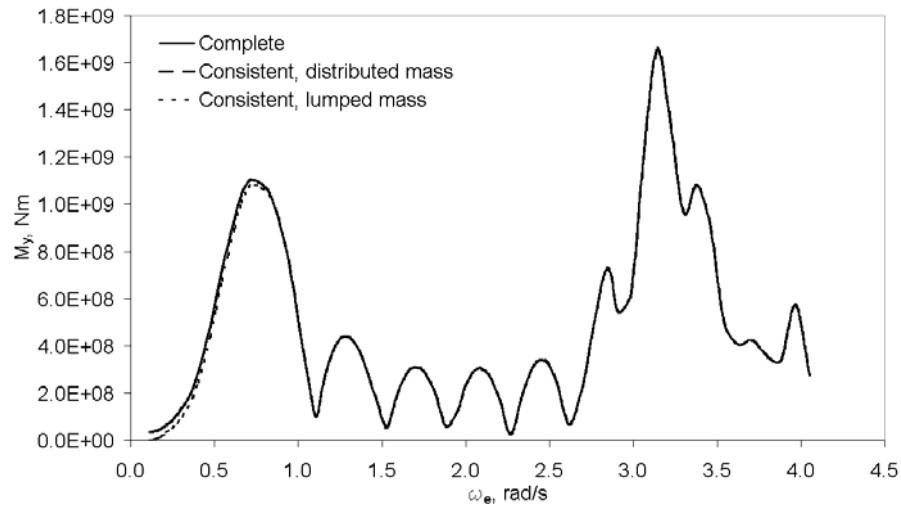


Figure 18 Transfer function of vertical bending moment at midship section, a 9415 TEU container ship, $\chi = 150^\circ$

Slika 18 Prijenosna funkcija vertikalnog momenta savijanja na sredini, brod za prijevoz kontejnera kapaciteta 9415 TEU, $\chi = 150^\circ$

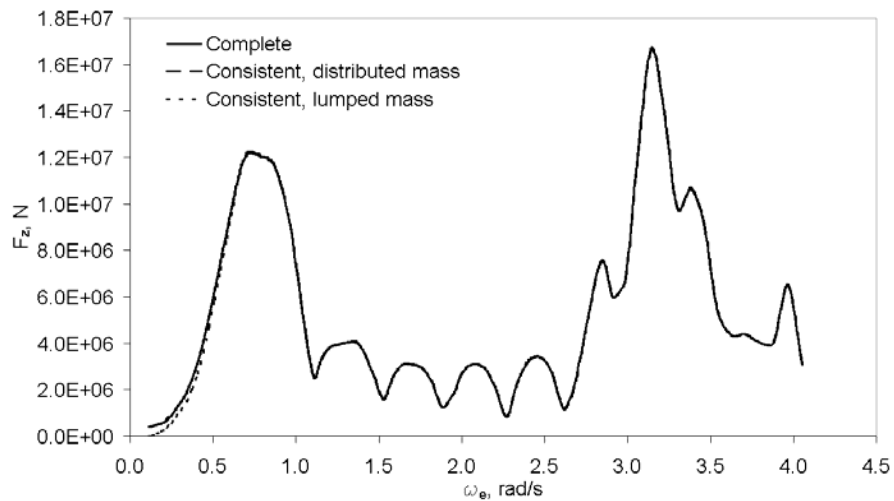


Figure 19 Transfer function of vertical shear force, a 9415 container ship, $\chi = 150^\circ$, $x = 85$ m

Slika 19 Prijenosna funkcija vertikalne smične sile, kontejnerski brod kapaciteta 9415 TEU

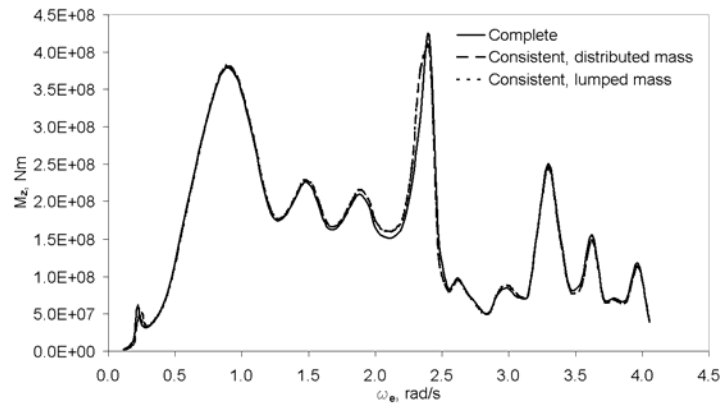


Figure 20 Transfer function of horizontal bending moment at midship section, a 9415 TEU container ship, $\chi = 150^\circ$

Slika 20 Prijenosna funkcija horizontalnog momenta savijanja na sredini, kontejnerski brod kapaciteta 9415 TEU, $\chi = 150^\circ$

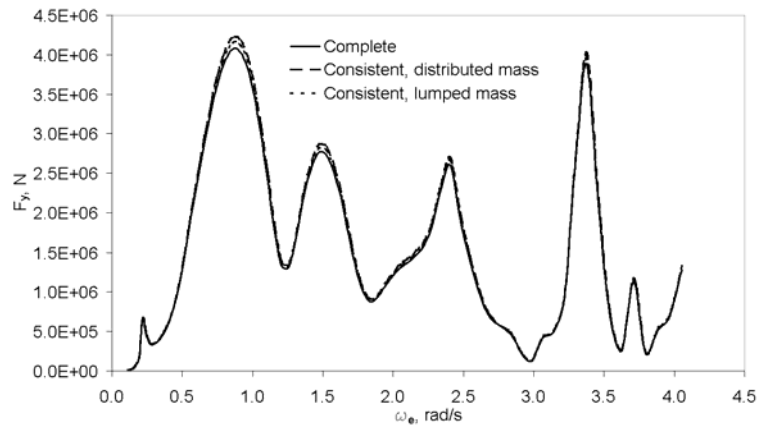


Figure 21 Transfer function of horizontal shear force, a 9415 TEU container ship, $\chi = 150^\circ$, $x = 85$ m

Slika 21 Prijenosna funkcija horizontalne smične sile, kontejnerski brod kapaciteta 9415 TEU, $\chi = 150^\circ$, $x = 85$ m

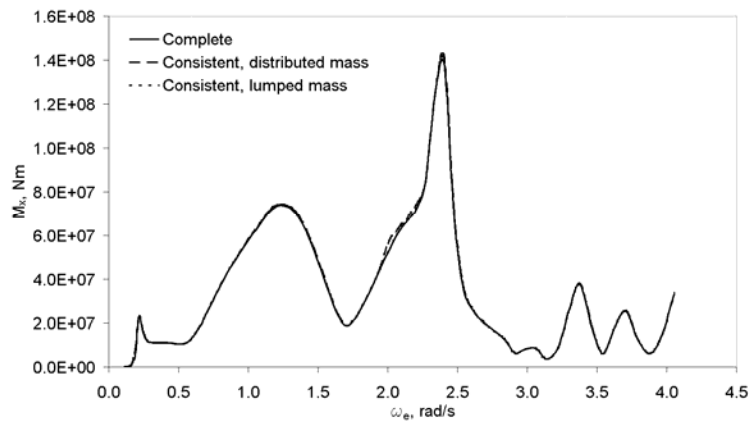


Figure 22 Transfer function of torsional moment at midship section, a 9415 TEU container ship, $\chi = 150^\circ$

Slika 22 Prijenosna funkcija momenta uvijanja na sredini, kontejnerski brod kapaciteta 9415 TEU, $\chi = 150^\circ$

In Figures 23 to 28 transfer functions of sectional forces determined by the ordinary procedure for rigid body motion and hydroelastic analysis with consistent restoring stiffness and distributed mass are shown. The rigid body values at resonant motions are somewhat lower than those of the elastic body. Resonances of elastic response are captured in the area of higher encounter frequencies where the ordinary procedure based on a ship as rigid body is not applicable.

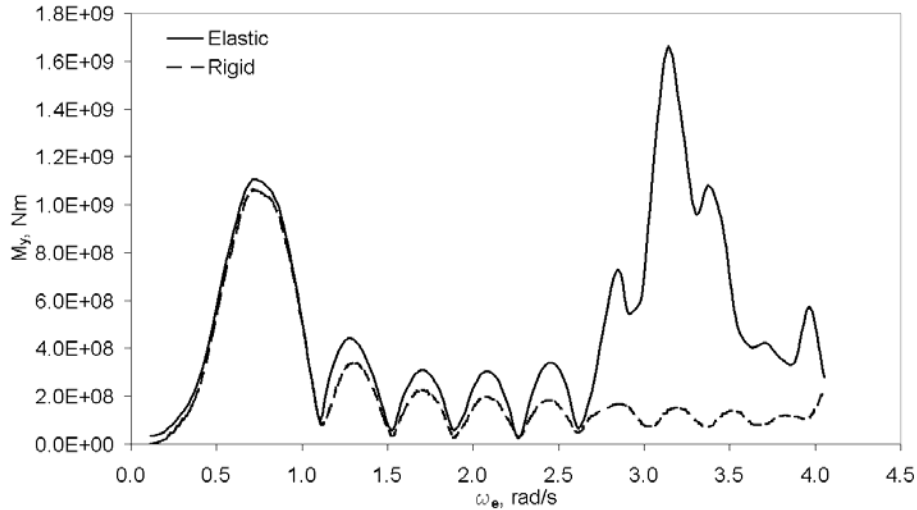


Figure 23 Transfer function of vertical bending moment for rigid and elastic ship at midship section, $\chi = 150^\circ$

Slika 23 Prijenosna funkcija vertikalnog momenta savijanja na sredini za kruti i elastični brod, $\chi = 150^\circ$

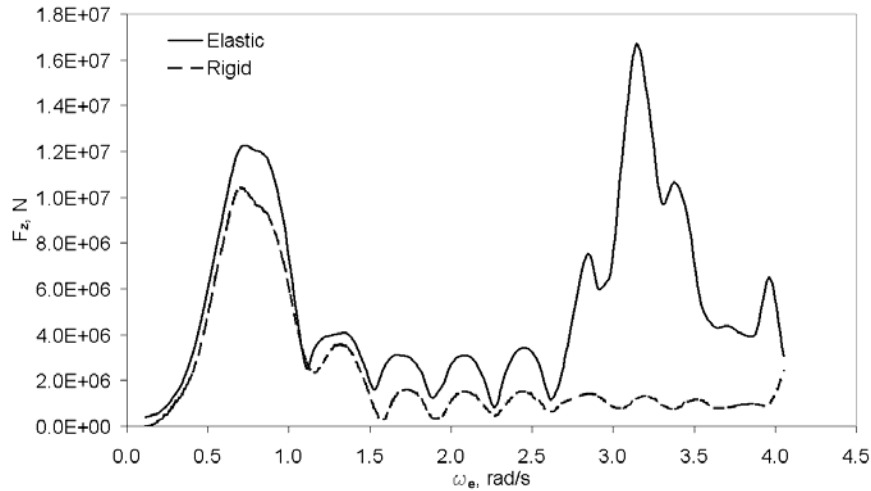


Figure 24 Transfer function of vertical shear force for rigid and elastic ship, $\chi = 150^\circ$, $x = 85$ m

Slika 24 Prijenosna funkcija vertikalne smične sile za kruti i elastični brod, $\chi = 150^\circ$, $x = 85$ m

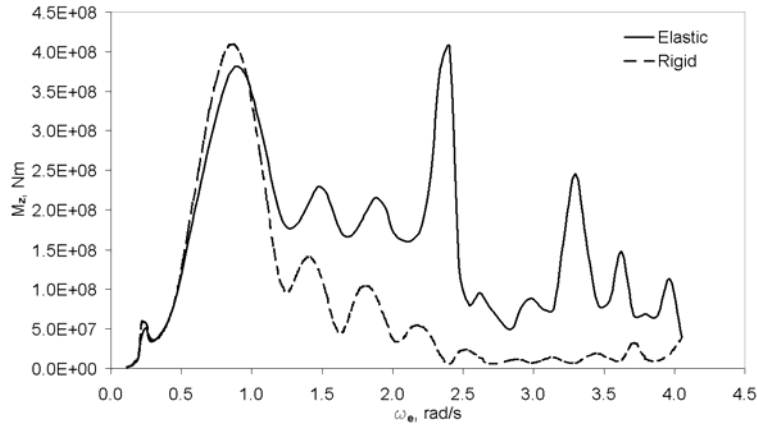


Figure 25 Transfer function of horizontal bending moment for rigid and elastic ship at midship section, $\chi = 150^\circ$

Slika 25 Prijenosna funkcija horizontalnog momenta savijanja na sredini za kruti i elastični brod, $\chi = 150^\circ$

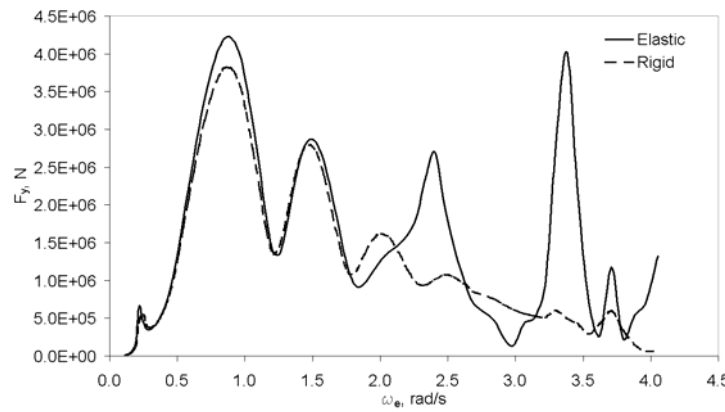


Figure 26 Transfer function of horizontal shear force for rigid and elastic ship, $\chi = 150^\circ$, $x = 35$ m

Slika 26 Prijenosna funkcija horizontalne smične sile za kruti i elastični brod, $\chi = 150^\circ$, $x = 35$ m

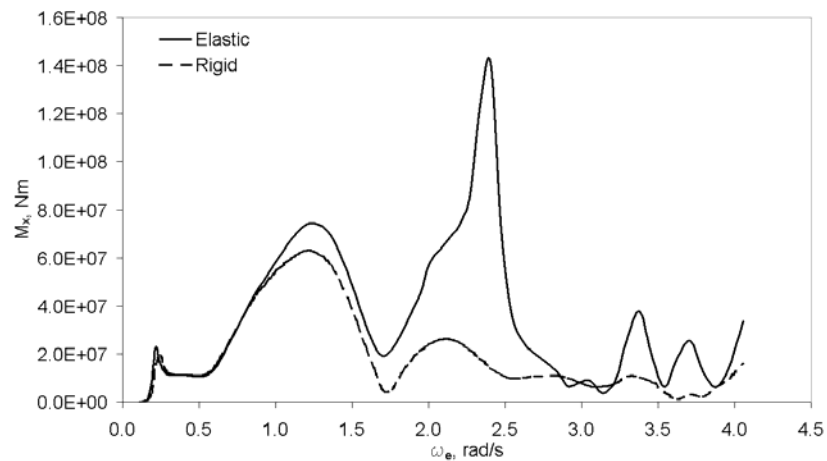


Figure 27 Transfer function of torsional moment for rigid and elastic ship at midship section, $\chi = 150^\circ$

Slika 27 Prijenosna funkcija momenta uvijanja na sredini za kruti i elastični brod, $\chi = 150^\circ$

7 Conclusion

One of unwanted physical phenomena related to modern container ships is springing, characterized as resonant motion, which manifests as periodic response to wave excitation. Adequate analysis of such physical phenomenon is provided by hydroelastic analysis that extends traditional seakeeping analysis to elastic modes.

Mathematical hydroelastic model consists of structural, hydrodynamic and hydrostatic models, and it is possible to formulate it on different levels of complexity, depending on a particular purpose. Restoring stiffness formulation, enclosed in the hydrostatic model, represents special problem due to disagreements related to certain restoring stiffness components definition and to the methodology of restoring stiffness analysis. Therefore, in order to ensure reliable problem description, it is necessary to develop mathematically and physically transparent restoring stiffness formulation.

This paper presents the theoretical improvement and formulation of restoring stiffness via finite element method, which is very useful for practical utilization because it enables the usage of 3D FEM model as integration domain within the hydrostatic model. The validity of the numerical procedure was demonstrated in the case of a prismatic barge with very good agreement between numerical and possible analytical values.

Restoring stiffness of ship structure was determined by program RESTAN using the modal displacements and stress distribution determined via commercial program NASTRAN. Total geometric stiffness was also determined by program RESTAN which comprises three parts related to both translatory and membrane displacements. The effect on the hydroelastic response was examined for three restoring stiffness formulations: consistent with distributed mass, consistent with lumped masses, and complete one. A good agreement was found between all results of the three formulations. Also, good agreement of the results was achieved in the case of rigid body modes where numerical and analytical values exist. The only exception is numerical instability of complete formulation in the case of roll.

Finally, it can be concluded that the restoring stiffness analysis using complete formulation is, although physically correct, very complex and extensive and does not result with expected accuracy improvement. Due to that fact this formulation is not suitable for the practical usage in shipping industry. On the other hand, consistent formulation with lumped mass is much simpler and gives very good results. Therefore, it can be recommended for the further utilization.

Acknowledgment

This investigation was carried out within the EU FP7 Project TULCS (Tools for Ultra Large Container Ships) and was supported by a National Research Foundation of Korea (NRF) grant funded by the Korea Government (MEST) through GCRC-SOP (Grant No. 2011-0030669). The authors express their gratitude to Fabien Bigot, *Bureau Veritas*, Paris, for numerical calculation of the barge and container ship hydrodynamic properties.

References

- [1] BISHOP, R. E. D., PRICE, W. G.: 'Hydroelasticity of Ships', Cambridge University Press, 1979.
- [2] PEDERSEN, P. T.: 'Torsional response of containerships', *Journal of Ship Research*, 29 (3), 1985, p. 194-205.
- [3] SNAME, 'Principles of Naval Architecture', Jersey City, 1988.
- [4] SENJANOVIĆ, I., MALENICA, Š., TOMAŠEVIĆ, S., RUDAN, S.: 'Methodology of ship hydroelasticity investigation', *Brodogradnja*, 58-2, 2007, p. 133 – 145.
- [5] MALENICA, Š.: 'Hydro-structure interactions in seakeeping', In: Terze, Z., Lacor, Ch. (Eds.), *Proceedings of the International Workshop on Coupled Methods in Numerical Dynamics CMWD*, 2007, p. 231 – 256.
- [6] PRICE, W. G., WU, Y.: 'Hydroelasticity of marine structures', in: *Theoretical and Applied Mechanics*, Eds. Niordson, F. I. and Olhoff, N., North-Holland, Elsevier Science Publishers, B. V, 1985, p. 311 – 370.
- [7] NEWMAN, J. N.: 'Wave effects on deformable bodies', *Applied Ocean Research* 16, 1994, p. 47 – 59.
- [8] RIGGS, H. R.: 'Hydrostatic stiffness of flexible floating structures', in: *Proceedings of International Workshop on Very Large Floating Structures*, Hayama, Japan, 1996, p. 229 – 34.
- [9] MALENICA, Š., MOLIN, B., REMY, F. SENJANOVIĆ, I.: 'Hydroelastic response of a barge to impulsive and non-impulsive wave loads', *Hydroelasticity in Marine Technology*, Oxford, UK, 2003, p. 107 – 115.
- [10] MOLIN, B.: 'Hydrostatique d'un corps deformable', Technical note, Ecole Superieure d'Ingenieurs de Marseille, Marseille, France, 2003.
- [11] BRONŠTEJN, I. N., SEMENDJAJEV, K. A.: 'Mathematical handbook', Tehnička knjiga, Zagreb, 1991, (in Croatian).
- [12] SENJANOVIĆ, I., MALENICA, Š., TOMAŠEVIĆ, S.: 'Hydroelasticity of large container ships', *Marine Structures* 22, 2009, p. 287-314.
- [13] HUANG, L. L., RIGGS, H. R.: 'Hydrostatic stiffness of flexible floating structures for linear hydroelasticity', *Marine Structures* 13, 2000, p. 91 - 106.
- [14] RIGGS, H. R.: 'Comparison of formulations for the hydrostatic stiffness of flexible structures', *ASME Journal of Offshore Mechanics and Arctic Engineering*, Vol. 131/024501, 2009.
- [15] SENJANOVIĆ, I., HADŽIĆ, N., TOMIĆ, M.: 'Investigation of restoring stiffness in the hydroelastic analysis of slender marine structures', *ASME Journal of Offshore Mechanics and Arctic Engineering*, Vol. 133/031107-1, 2011.
- [16] HADŽIĆ, N.: 'Restoring stiffness in hydroelastic analysis of ship structures', Ph.D. Thesis, FAMENA, 2012, University of Zagreb, Zagreb (in Croatian).
- [17] SENJANOVIĆ, I., HADŽIĆ, N., BIGOT, F.: 'Finite element formulation of different restoring stiffness issues in the ship hydroelastic analysis and their influence on response', *Ocean Engineering*, (accepted for publishing).
- [18] SENJANOVIĆ, I., VLADIMIR, N., TOMIĆ, M.: 'Formulation of consistent restoring stiffness in ship hydroelastic analysis', *Journal of Engineering Mathematics* 72, 2012, p. 141 - 157.

- [19] SENJANOVIĆ, I., TOMAŠEVIĆ, S., VLADIMIR, N., TOMIĆ, M., MALENICA, Š.: ‘Ship hydroelastic analysis with sophisticated beam model and consistent restoring stiffness’, *Hydroelasticity in Marine Technology*, University of Southampton, UK, 2009.
- [20] TUITMAN, J. T., MALENICA, Š.: ‘Fully coupled seakeeping, slamming and whipping’, *Journal of Engineering for Maritime Environment*, Vol. 223, No M3, 2009, p. 439 - 456 (A special issue in honour of Professor W. Geraint Price).
- [21] RIGGS, H. R., NIIMI, K. M., HUANG, L. L.: ‘Two benchmark problems for three-dimensional, linear hydroelasticity’, *ASME Journal of Offshore Mechanics and Arctic Engineering*, Vol. 129, 2007, p. 149 - 157.
- [22] SENJANOVIĆ, I., HADŽIĆ, N., VLADIMIR, N.: ‘Restoring stiffness in hydroelastic analysis of marine structures’, *Brodogradnja 62-3*, 2011, p. 265 - 279.
- [23] SENJANOVIĆ, I., HADŽIĆ, N., TOMIĆ, M., MALENICA, Š.: ‘On consistency of actual restoring stiffness formulations in hydroelastic analysis of marine structures’, *IWWWFB*, Athens, 2011.
- [24] MALENICA, Š., TUITMAN, J. T., BIGOT, F., SIRETA, F. X.: ‘Some aspects of 3D linear hydroelastic models of springing’, *International Conference on Hydrodynamics*, Nantes, 2008.
- [25] ZIENKIEWICZ, O. C.: ‘The Finite Element Method in Engineering Science’, McGraw– Hill, London, 1971.
- [26] BIGOT, F.: ‘WP4: Global hydro elastic loading & responses – D4.3: Interface module for coupling 3D FEM structural model to 3D hydrodynamic model’, FP7 TULCS project, Bureau Veritas, Paris, 2010.
- [27] SENJANOVIĆ, I., VLADIMIR, N., HADŽIĆ, N.: ‘Some aspects of geometric stiffness modeling in hydroelastic analysis of ship structures’, *Transactions of FAMENA XXXIV – 4*, 2010.
- [28] MSC. NASTRAN 2005, *Installation and Operation Guide*, MSC. Software, 2005.
- [29] HYDROSTAR, *User’s Manual*, Bureau Veritas, Paris, 2006.